



**HAL**  
open science

# Viability approach to Hamilton-Jacobi-Moskowitz problem involving variable regulation parameters

Anna Desilles

► **To cite this version:**

Anna Desilles. Viability approach to Hamilton-Jacobi-Moskowitz problem involving variable regulation parameters. Mathematics of Traffic Flow Modeling, Estimation and Control, Dec 2011, Los Angeles, United States. hal-00756895

**HAL Id: hal-00756895**

**<https://hal.science/hal-00756895>**

Submitted on 23 Nov 2012

**HAL** is a multi-disciplinary open access archive for the deposit and dissemination of scientific research documents, whether they are published or not. The documents may come from teaching and research institutions in France or abroad, or from public or private research centers.

L'archive ouverte pluridisciplinaire **HAL**, est destinée au dépôt et à la diffusion de documents scientifiques de niveau recherche, publiés ou non, émanant des établissements d'enseignement et de recherche français ou étrangers, des laboratoires publics ou privés.

# Viability approach to Hamilton-Jacobi-Moskowitz problem involving variable regulation parameters

Anna Désilles  
ENSTA Paristech, Paris, France

April 30, 2012

## Abstract

We present a few applications of the viability theory to the solution to the Hamilton-Jacobi-Moskowitz problems when the Hamiltonian (fundamental diagram) depends on time, position and/or some regulation parameters. We study such a problem in its equivalent variational formulation. In this case, the corresponding lagrangian depends on the state of the characteristic dynamical system. As the Lax-Hopf formulae that give the solution in a semi-explicit form for an homogeneous lagrangian do not hold, we use a capture basin algorithm to compute the Moskowitz function as a viability solution of the Hamilton-Jacobi-Moskowitz problem with general conditions (including initial, boundary and internal conditions). We present two examples of applications.

In the first one we introduce the variable speed limit as a regulation parameter. Our approach allows to compute the Moskowitz function for all values of the variable speed limit in a selected range and then to analyze its influence on the traffic flow. In particular, we study the case when the variation of the speed limit is applied locally, in space and time.

Our second example deals with the local load capacity variations on the road. Such a variation can be a permanent property of the road (road narrowing) or it can be due to a temporary change of number of lanes (an accident or roadworks, for example). One can also use it as a regulation parameter by variable assignment of a supplementary lane.

# 1 Introduction

In this paper we focus on macroscopic modeling of traffic flow. Consider a straight road with a single lane.

In the macroscopic modeling framework, related with the theory of incompressible flow, the traffic is considered as a continuum medium and is described by the following three quantities:

- $k(t, x)$ , the density, measured in vehicles per unit of length;
- $q(t, x)$ , the flux, measured in vehicles per unit of time;
- $v(t, x)$ , the mean speed.

These quantities are defined in such a way that they are related by the expression:

$$q(t, x) = v(t, x)k(t, x)$$

The start point of this work is the well known Lighthill-Whitham-Richards (LWR) ([16], [18]) based on the assumption that there exists a relationship between two of three macroscopic characteristics of the traffic that is an intrinsic property of the road. This relationship is called "fundamental diagram". For example, it is often represented as a "flow-density" relation:

$$q(t, x) = h(k(t, x), x, t)$$

In general, it is assumed that the fundamental diagram does not depend on time  $t$  or space  $x$ :

$$q = h(k)$$

This assumption simplifies many theoretical and numerical considerations. It can be justified in practice if we study the traffic situation for a short time period and that if the considered road section has no structural change that can lead to a different fundamental diagram. However, in some cases the fundamental diagram can depend on the time and space. It also depends on a number of parameters considered as being intrinsic (maximum speed, maximum capacity) and that could be useful to control the traffic flow in order to reduce the congestion.

In this paper an LWR model with a non homogeneous fundamental diagram is studied. Originally, the LWR model is formulated as a conservation law with some initial and boundary conditions. It is well known that such problems are difficult to solve analytically and numerically because of presence of shocks. To avoid these difficulties we state the problem in an integrated form, as a Hamilton-Jacoby type equation (see [6], [7], [8], [15]). We use the viability theory framework to define and compute the solution of such problems. The viability solution of a general class of first order hyperbolic problems, such as Hamilton-Jacobi equations, is defined in [2]. This concept allows to give sense to a solution of the problem with a very general conditions including boundary, initial and lagrangian (or internal) conditions. For the traffic problems with homogeneous fundamental diagram, the viability theory was applied in [6, 7, 8, 15]. In particular, there exists a semi explicit form of the solution given by a Lax-Hopf formula. This fact was used in [6], [7], [8] to develop fast numerical computations for traffic analysis. This technique was also extended to some special cases of non homogeneous fundamental diagrams in [5].

The present work extends the definition of the viability solutions for the problems with non homogeneous fundamental diagram. This solution can be characterized as a value function

of some variational problem under very general assumptions. Unfortunately, the Lax-Hopf representations do not hold for the problems with non homogeneous hamiltonians. One can still use the viability capture basin algorithm to compute numerical approximations of the solutions. Some examples are given at the end of this article.

## 2 The Hamilton-Jacobi-Moskowitz PDE

### 2.1 Problem statement

Consider a straight road with a single lane. Assume that the vehicles cannot pass each other. It is represented by an interval  $[0, x_{max}]$ . We can also choose  $] - \infty, +\infty[$ . If there is multiple lanes, we consider that the effects of changes of lanes are neglected.

We focus here on the case when the fundamental diagram depends on time and space and, eventually, some regulation parameters. Assume that the fundamental diagram is of the form

$$q = h(k, t, x, a)$$

where  $a = (a_1, \dots, a_r) \in A \subset \mathbb{R}^r$  are some given parameters and consider the traffic function  $V = V(t, x, a)$  as function of these parameters.

**Definition 1. [Traffic Function]** A differentiable traffic function  $V : (t, x, a) \mapsto V(t, x, a)$  is a function such that it's first derivatives with respect to time and to position are respectively regarded as a flow and a density:

$$q(t, x, a) = \frac{\partial V(t, x, a)}{\partial t} \quad k(t, x, a) = -\frac{\partial V(t, x, a)}{\partial x}$$

When the traffic function is not differentiable, one can still define generalized gradients  $(p_t, p_x) \in \partial_- V(t, x, a)$  representing pairs of flows and densities at  $(t, x)$ . This function is also called "Moskowitz function" or "cumulated number function" in the literature [15]. The traffic function has different physical interpretations:

$$\left\{ \begin{array}{l} (i) \quad V(t, x, a) - V(t, \bar{\gamma}, a) := -\int_x^{\bar{\gamma}} \frac{\partial V(t, \xi, a)}{\partial x} d\xi \\ \quad \text{is the incremental congestion on the interval } [x, \bar{\gamma}] \text{ at time } t \\ \quad \text{representing the "cumulated vehicle count" after position } x \\ (ii) \quad V(t, x, a) - V(d, x, a) := \int_d^t \frac{\partial V(\tau, x, a)}{\partial t} d\tau \\ \quad \text{is the incremental congestion on the interval } [d, t] \text{ at position } x \\ (iii) \quad V(t, x, a) - V(d, \xi(d), a) := \int_d^t \frac{dV(\tau, \xi(\tau), a)}{dt} d\tau \\ \quad \text{is the incremental congestion on the interval } [d, t] \\ \quad \text{along an evolution } \xi(\cdot) \text{ arriving at } x \text{ at time } t: \xi(t) = x \end{array} \right. \quad (2.1)$$

Using the first interpretation one can identify the trajectories of individual vehicles as the ones over which the Moskowitz function is constant.

**Definition 2. [The Fundamental Diagram]**

The fundamental diagram of transportation engineering is the graph  $\text{Graph}(\mathbf{h})$  of a density-flow function  $\mathbf{h}$  associating with each density a flow.

The function  $\mathbf{h}$  is the "Hamiltonian" governing the evolution of the traffic function through the Moskowitz partial differential equation

$$\frac{\partial V(t, x, a)}{\partial t} = \mathbf{h} \left( t, x, -\frac{\partial V(t, x, a)}{\partial x}, a \right)$$

In the Moskowitz framework, the Hamiltonian  $\mathbf{h} : \mathbb{R} \mapsto \mathbb{R}$  is assumed to be a concave density-flow function vanishing at 0-density and at the given capacity density  $\omega > 0$ :

$$\begin{cases} (i) & \mathbf{h}(t, x, 0, a) = 0 \text{ and} \\ (ii) & \mathbf{h}(t, x, \omega, a) = 0 \end{cases} \quad (2.2)$$

## 2.2 Traffic Conditions

Let  $\mathbf{c} : (t, x, a) \mapsto \mathbf{c}(t, x, a) \in \mathbb{R}_+ \cup \{+\infty\}$  be a given function, *decreasing with position,  $x$ , and increasing with time  $t$* . The subset  $\mathbf{C}(t, a)$  is the domain of the traffic profile  $x \mapsto \mathbf{c}(t, x, a)$  (which is thus finite for all  $x \in \mathbf{C}(t, a)$ ). The traffic conditions can be expressed as the following requirement for the traffic function

$$\forall x \in \mathbf{C}(t, a), \quad V(t, x, a) \leq \mathbf{c}(t, x, a) \quad (2.3)$$

We associate with this condition the *traffic domain map*  $t \rightsquigarrow \mathbf{C}(t, a)$ , which is the set-valued map defined by

$$\mathbf{C}(t, a) := \{x \text{ such that } \mathbf{c}(t, x, a) < +\infty\} \quad (2.4)$$

These general traffic conditions cover the following classical and less classical examples:

1. *Maximum congestion threshold*  $(t, x, a) \mapsto \gamma^\sharp(t, x, a)$  setting an upper bound on the congestion of traffic by requiring that

$$V(t, x, a) \leq \gamma^\sharp(t, x, a)$$

2. *Dirichlet boundary conditions* defined on the boundary of the domain. In this case, we set  $\mathbf{c}(0, x, a) := \gamma_0(x, a)$  and  $\mathbf{c}(t, x, a) = +\infty$  whenever  $t > 0$ . Hence  $\mathbf{C}(0, a) = \text{Dom}(\gamma_{0,a})$  and  $\mathbf{C}(t, a) = \emptyset$ ;
3. *Eulerian conditions* measuring at each time the cumulative number of vehicles at *fixed* locations;
4. *Lagrangian "mobile" conditions* measuring few vehicle evolutions  $t \mapsto \gamma_i(t)$  during some time intervals  $]\underline{\tau}_i, \bar{\tau}_i]$  (by tracking probe vehicles).

In the case of a finite number of Lagrangian conditions,  $\mathbf{C}(t, a) = \bigcup_i \text{such that } \underline{\tau}_i \leq t \leq \bar{\tau}_i \{ \gamma_i(t) \}$  and the traffic condition  $\mathbf{c}(t, \gamma_i(t), a)$  is defined on the graphs  $(t, \gamma_i(t))_{t \geq 0}$  of the evolution of each vehicle  $i$ .

**Definition 3.** [*The Hamilton-Jacobi-Moskowitz Problem*] *The complete model takes into account the two above requirements on the congestion function  $V$ :*

$$\begin{cases} (i) & \forall t > 0, \forall x \notin \mathbf{C}(t), \quad a \in \mathcal{A}, \quad \mathbf{h} \left( -\frac{\partial V(t, x, a)}{\partial x}, t, x, a \right) = \frac{\partial V(t, x, a)}{\partial t} \\ (ii) & \forall t > 0, \forall x \in \mathbf{C}(t), \quad a \in \mathcal{A}, \quad V(t, x) \leq \mathbf{c}(t, x, a) \end{cases} \quad (2.5)$$

### 2.3 Viability solution of the Hamilton-Jacobi-Moskowitz Problem

In what follows we introduce the viability characterization of the Barron-Jensen/Frankoska ([4], [12]) solution of the the Hamilton-Jacobi-Moskowitz Problem 2.5. In this purpose we first recall some basic definitions from the viability theory (see [3],[1] for more details).

Consider a set-valued map  $F : \mathbb{R}^n \rightsquigarrow \mathbb{R}^n$  that associates to each  $x \in \mathbb{R}^n$  an nonempty set  $F(x) \neq \emptyset$  and a differential inclusion associated with it:

$$x'(t) \in F(x(t)), \quad t > 0. \quad (2.6)$$

Assume that

**(HF1)**  $F$  is Lipschitz continuous

**(HF1)**  $F$  has non empty, convex, closed images

Let  $x \in \mathbb{R}^d$ . We denote by

$$S_F(x) = \{y(\cdot), \text{ absolutely continuous, such that } y(0) = x \text{ and } \forall t > 0 \ y'(t) \in F(y(t))\}$$

the set of all trajectories starting at  $x$  and governed by (2.6).

Let  $\mathcal{C} \subset \mathbb{R}^n$  be a compact set that represents a target and  $\mathcal{K} \subset \mathbb{R}^n$  be a closed subset representing the state constraints.

**Definition 4.** A trajectory  $y(\cdot) \in S_F(x)$  starting at  $x \in \mathbb{R}^n$  is viable in  $\mathcal{K}$  until a time  $T > 0$  if

$$\forall s \in [0, T[, \quad y(s) \in \mathcal{K}.$$

Let denote by

$$\mathcal{V}(x, \mathcal{K}, T) = \{y(\cdot) \in S_F(x) \mid \forall s \in [0, T[, \quad y(s) \in \mathcal{K}\}$$

the set of all viable trajectories starting at  $x \in \mathbb{R}^d$ .

**Definition 5.** The capture basin for the differential inclusion 2.6 is the set of initial states from which the set  $\mathcal{C}$  is reachable :

$$Capt_F(\mathcal{C}, \mathcal{K}) := \left\{ x \in \mathbb{R}^d \mid \exists T > 0, \exists y(\cdot) \in \mathcal{V}(x, \mathcal{K}, T), y(T) \in \mathcal{C} \right\} \quad (2.7)$$

Let associate with the Hamilton-Jacobi-Moskowitz Problem 2.5 an auxiliary dynamical system using the the Lagrange-Fenchel transform of  $h(p)$ :

**Definition 6.** [The Celerity Diagram] The celerity diagram is the function  $\mathbf{l}$  defined by

$$\forall (u), \quad \mathbf{l}(t, x, u, a) := \sup_{(p)} [\mathbf{h}(t, x, p, a) - \langle p, u \rangle] \quad (2.8)$$

It's graph  $\text{Graph}(\mathbf{l})$  is called the fundamental celerity diagram.

Consider the following *characteristic dynamical system*

$$\left\{ \begin{array}{l} (i) \quad \tau'(t) = -1 \\ (ii) \quad \xi'(t) = -u \\ (iv) \quad \eta'(t) = -\mathbf{l}(u, \tau, x, \alpha) \\ (iii) \quad \alpha'(t) = 0 \end{array} \right. \quad (2.9)$$

controlled by celerity  $u(\cdot)$ .

**Definition 7.** [ *Viability Solution to the Moskowitz Problem* ] Let us consider the epigraph  $\mathcal{E}p(\mathbf{c})$  of the traffic condition  $\mathbf{c}$ . The viability solution (associated with the traffic condition  $\mathbf{c}$ )  $V$  to the Moskowitz problem ( 2.5) is defined by the following formula

$$V(T, x, a) := \inf_{(T, x, y, a) \in \text{Capt}_{(2.9)}(\mathbb{R}_+ \times \mathbb{R} \times \mathbb{R} \times \mathbb{R}, \mathcal{E}p(\mathbf{c}))} y \quad (2.10)$$

**Theorem 1.** [ *Barron-Jensen/Frankowska Viscosity Solution* ] . For any semicontinuous traffic condition  $c$  the viability solution defined by 2.10 is the unique function  $V$  satisfying the following conditions

$$V(t, x, a) \leq \mathbf{c}(t, x, a)$$

Hamilton-Jacobi-Moskowitz PDE 2.5 in the sense that

$$\left\{ \begin{array}{l} (i) \quad \text{if } V(t, x, a) < \mathbf{c}(t, x, a), \text{ then} \\ \quad \forall (p_t, p_x) \in \partial_{t,x} V(t, x, a), \quad p_t + \mathbf{h}(t, x, -p_x, a) = 0 \\ (ii) \quad \text{if } V(t, x) \leq \mathbf{c}(t, x), \text{ then} \\ \quad \forall (p_t, p_x) \in \partial_{t,x} V(t, x, a), \quad p_t + \mathbf{h}(t, x, -p_x, a) \leq 0 \end{array} \right. \quad (2.11)$$

which is the very definition of a Barron-Jensen/Frankowska viscosity solution for lower semicontinuous functions.

## 2.4 Variational formulation of the problem

The variational formulation of the problem was first studied by Daganzo in [9, 10]. For the viability solution that we consider in this paper the variational principle is the more natural formulation. Let  $T > 0$  and  $d \in [0, T]$  be a given departure time. Denote by

$$\mathcal{A}(d, T; x) = \{ \xi(\cdot), \text{ absolutely continuous on } [d, T], \xi(d) \in \mathbf{C}(d), \xi(T) = x \}$$

the set of all absolutely continuous evolutions starting at the time  $d$  and arriving at the time  $T$  in  $x$ .

Let  $\xi(\cdot) \in \mathcal{A}(d, T; x)$  be such an evolution. We associate with each departure time  $d \in [0, T]$  the minimal *travel traffic value* over the traffic evolutions  $\xi(\cdot) \in \mathcal{A}(d, T; x)$  defined on the travel interval  $[d, T]$ , defined by

$$J(d, T; x, a) := \inf_{\xi(\cdot) \in \mathcal{A}(d, T; x)} \left( \int_d^T \mathbf{l}(\tau, x, \xi'(\tau), a) d\tau + \mathbf{c}(d, \xi(d), a) \right)$$

The celerity function  $\mathbf{l}$  plays the role of a *Lagrangian* in the variational formulation:

**Theorem 2.** [*Congestion Variational Principle*] The viability solution  $V(t, x, a)$  to the traffic problem ( 2.5), minimizes the travel traffic value with respect to departure time  $d$  and evolutions  $\xi(\cdot) \in \mathcal{A}(d, T; x)$ :

$$\begin{cases} V(T, x, a) = \inf_{d \in [0, T]} J(d, T; x, a) \\ = \inf_{d \in [0, T]} \inf_{\xi(\cdot) \in \mathcal{A}(d, T; x)} \left( \int_d^T \mathbf{l}(\tau, x, \xi'(\tau), a) d\tau + \mathbf{c}(d, \xi(d), a) \right) \end{cases} \quad (2.12)$$

Alternatively, one can formulate this variational principle in terms of the celerity  $u(\cdot)$  instead of traffic evolutions  $\xi \in \mathcal{A}(d, T; x)$ :  $V(T, x, a) =$

$$\inf_{u(\cdot) \in L^1(0, T; \text{Dom}(\mathbf{l})), t^* \in [0, T]} \left( \int_0^{t^*} \mathbf{l}(\tau, x, u(\tau), a) d\tau + \mathbf{c} \left( T - t^*, x - \int_0^{t^*} u(\tau) d\tau \right) \right) \quad (2.13)$$

This theorem is the direct consequence of the general result in Chapter 13 of [2].

### 3 Numerical solution

To compute the solution numerically, we use the capture basin algorithm for epigraphs. The new implementation that we present here uses the equivalence between a capture basin and a backward reachable set. Consider a differential inclusion ( 2.6). Let  $K \subset \mathbb{R}^n$  and  $B \subset K$  be closed sets. We call reachable set from  $B$  under the dynamics  $F$  the set of all states in  $K$  that can be reached by an evolution starting in the set  $B$ :

$$\text{Reach}_F(B, K) := \left\{ z \in \mathbb{R}^n \mid \exists \tau \in [0, T], \exists x \in B, \exists y(\cdot) \in \mathcal{V}(x, K, \tau), \text{ s.t. } y(\tau) = z \right\} \quad (3.14)$$

It can be easily shown that

$$\text{Capt}_F(K, C) = \text{Reach}_{-F}(C, K) \quad (3.15)$$

To compute an approximation of the reachable set for the differential inclusion

$$x' \in -F(x)$$

we define a discrete-time dynamical system

$$\begin{cases} x_{n+1} \in G_\rho(x_n), & x_n \in K \\ x_0 \in K \end{cases} \quad (3.16)$$

where  $G_\rho$  is a set valued application associated with a chosen discretization scheme. The most popular (see []) is the explicit Euler scheme defined as follows:

$$G_\rho^E(x) = x - \rho F(x) \quad (3.17)$$

Following the recent results of [] we have used the Runge-Kutta approximation for the backward dynamical system:

$$G_\rho^{RK2}(x) = x - \rho F(x - 0.5\rho F(x)) \quad (3.18)$$

The reachable set for the backward dynamics is computed using the following recursive procedure

$$\begin{aligned} R_0 &= C; \\ R_{k+1} &= R_k \cup G_\rho(R_k \setminus R_{k-1}), k = 1, \dots \end{aligned} \quad (3.19)$$

The algorithm stops when  $R_{k+1} = R_k$ . This approach allows us to reduce a computational effort. Indeed, at each iteration, we compute only the image by  $G_\rho$  of the set  $R_k \setminus R_{k-1}$  which contains only the points added to the reachable set on previous step.

## 4 Numerical examples

In this section we present some numerical examples.

### 4.1 Fundamental diagrams

We have used three types of fundamental diagrams in our test. For all of them we have fixed some parameters:

- the free flow speed  $\nu = 3.0$  units of length/per units of time;
- the maximal (or jam) density  $\omega = 4.0$ .

#### 4.1.1 Triangular diagram

$$h(\nu, \omega, p) = \begin{cases} \nu p & \text{if } 0 \leq p \leq \frac{\omega}{2} \\ \nu(\omega - p) & \text{if } \frac{\omega}{2} < p \leq \omega \end{cases} \quad (4.20)$$

The critical density in this case is

$$\beta = \frac{\omega}{2}, \quad \delta = \sup_{p \in [0, \omega]} h(p) = h(\beta) = \frac{\nu\omega}{2}$$

and the diagram verifies the following :

$$h(0) = h(\omega) = 0; \quad h'(0) = \nu, \quad h'(\omega) = -\nu. \quad (4.21)$$

Its Legendre-Fenchel transform is

$$l(\nu, \omega, u) = \frac{\omega}{2}(\nu - u), \quad u \in [-\nu, \nu] \quad (4.22)$$

#### 4.1.2 Greenshields' diagram

This diagram was proposed by Greenshields in 1934 ([14]), based on a simple speed-density linear relationship.

$$h(\nu, \omega, p) = \frac{\nu}{\omega} p(\omega - p), \quad p \in [0, \omega] \quad (4.23)$$

The critical density in this case is

$$\beta = \frac{\omega}{2}, \quad \delta = \sup_{p \in [0, \omega]} h(p) = h(\beta) = \frac{\nu\omega}{4}$$

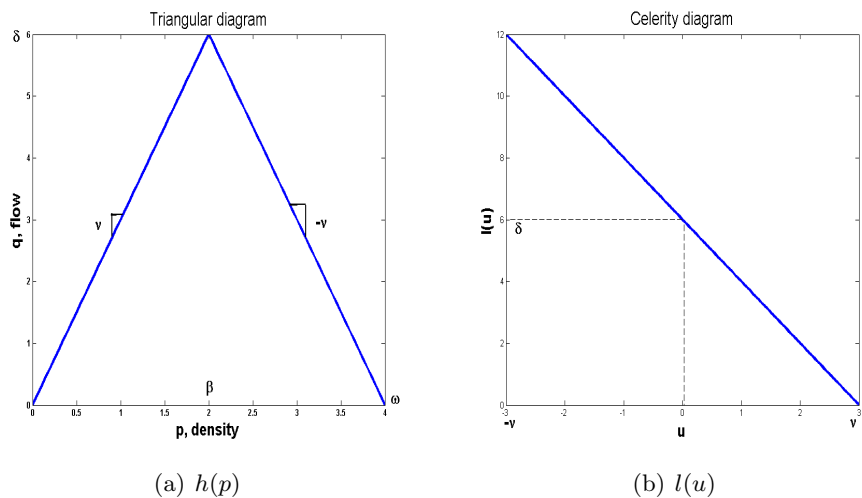


Figure 1: Triangular fundamental diagram

and the diagram verifies the following :

$$h(0) = h(\omega) = 0; \quad h'(0) = \nu, \quad h'(\omega) = -\nu. \quad (4.24)$$

Its Legendre-Fenchel transform is

$$l(\nu, \omega, u) = \frac{\omega}{4\nu}(\nu - u)^2, \quad u \in [-\nu, \nu] \quad (4.25)$$

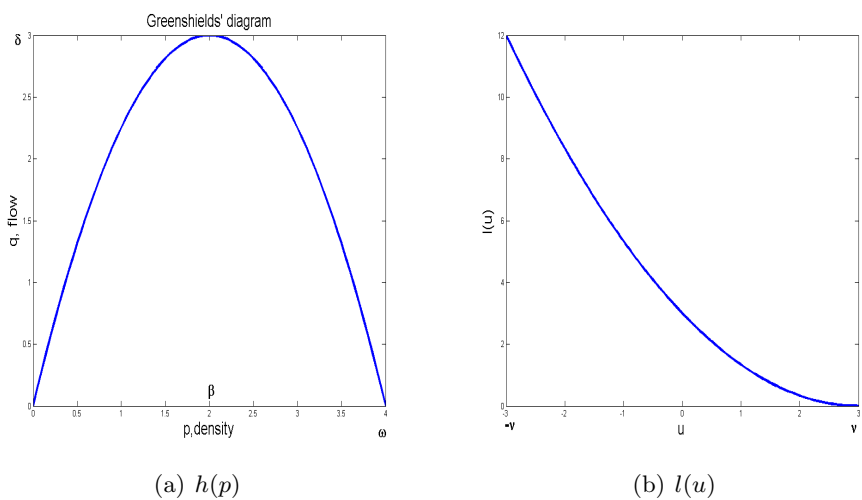


Figure 2: Greenshield's fundamental diagram

### 4.1.3 Edie's two regime diagram

This diagram was proposed by Edie in 1961 ([11]). It is a combination of the Greenberg [13] logarithmic model for high densities and of the Underwood [19] exponential model for low densities.

$$h(\nu, \omega, p) = \left\{ \begin{array}{ll} \nu p e^{-\frac{p \cdot e}{\omega}} & \text{if } 0 \leq p \leq \frac{\omega}{e} \\ \frac{\nu}{e} p \ln\left(\frac{\omega}{p}\right) & \text{if } \frac{\omega}{e} < p \leq \omega \end{array} \right\} \quad (4.26)$$

The critical density in this case is

$$\beta = \frac{\omega}{e}, \quad \delta = \sup_{p \in [0, \omega]} h(p) = h(\beta) = \frac{\nu \omega}{e^2}$$

and the diagram verifies the following :

$$h(0) = h(\omega) = 0; \quad h'(0) = \nu, \quad h'(\omega) = -\frac{\nu}{e}. \quad (4.27)$$

Its Legendre-Fenchel transform cannot be expressed analytically. The figure 3 shows (at right) it's numerical approximation.

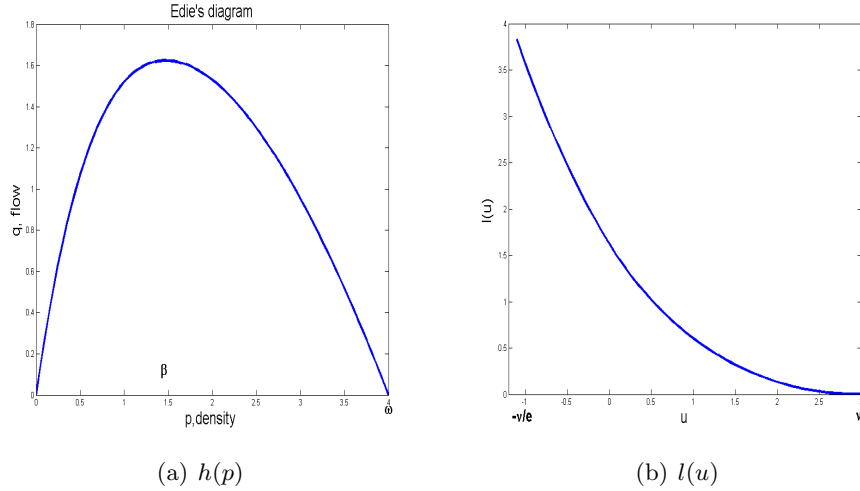


Figure 3: Edie's two regime fundamental diagram

### 4.1.4 Newell's diagram

This diagram was derived by Newell in 1961 ([17]) from a first-order car-following model.

$$h(\nu, w, \omega, p) = \nu p \left( 1 - e^{-\omega \frac{w}{\nu} \left( \frac{1}{p} - \frac{1}{\omega} \right)} \right), \quad p \in [0, \omega] \quad (4.28)$$

The diagram verifies the following :

$$h(0) = h(\omega) = 0; \quad h'(0) = \nu, \quad h'(\omega) = -w. \quad (4.29)$$

Its Legendre-Fenchel transform cannot be expressed analytically. The figure 4 shows (at right) it's numerical approximation.

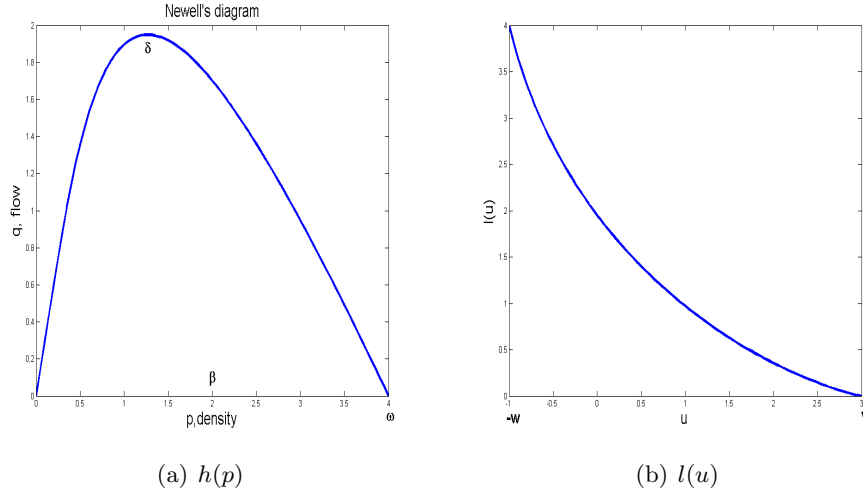


Figure 4: Newel's fundamental diagram

## 4.2 Investigation of the variable speed limit as a regulation parameter

In all considered diagrams the free-flow speed,  $\nu$  is a fixed parameter. Some other macroscopic characteristics of the traffic flow depend on it. In particular, the speed of the backward propagation of the information in the case of a bottleneck. It was shown in many works that the variation of the speed limit is an important factor of homogenization of the traffic. We show here how the viability theory allows us to integrate the speed variation into the macroscopic traffic model and to investigate its effect.

### 4.2.1 A slow vehicle impact with variable speed limits

Consider a road section  $[0, 6]$  with a constant initial concentration  $C_0 = 1.5$ . Assume that a slow vehicle enters the road at the initial time  $t_0 = 0$  and at the position  $x_0 = 3.5$  and that it moves with a constant velocity  $v_0 = 1.0$  until the time  $t_1 = 2.5$  when it leaves the road. Assume also that the concentration at the position  $x = 0$  remains constant, equal to  $C_0 = 1.5$  all the time. Consider the triangular fundamental diagram (4.20) for this example. The resulting traffic function is the solution of the problem (2.5) with the following target function  $c$ :

$$c(t, x) = \min(c_0(t, x), c_d(t, x), c_l(t, x)) \quad (4.30)$$

where

- the function  $c_0(t, x)$  corresponds to the initial condition

$$c_0(t, x) = \begin{cases} C_0(6.0 - x), & \text{if } t == 0 \\ +\infty, & \text{otherwise} \end{cases} \quad (4.31)$$

- the function  $c_d(t, x)$  corresponds to the boundary condition

$$c_d(t, x) = \begin{cases} 6C_0 + t \cdot h(C_0), & \text{if } x == 0 \\ +\infty, & \text{otherwise} \end{cases} \quad (4.32)$$

- the function  $c_l(t, x)$  corresponds to the langrangian condition

$$c_l(t, x) = \begin{cases} C_0(6.0 - x_0), & \text{if } t \in [0, 2.5], \quad x = x_0 + t \\ +\infty, & \text{otherwise} \end{cases} \quad (4.33)$$

The figure 5 shows, at the left, the traffic function computed by the viability algorithm and at the right the isolines ( that one can consider as a trajectories).

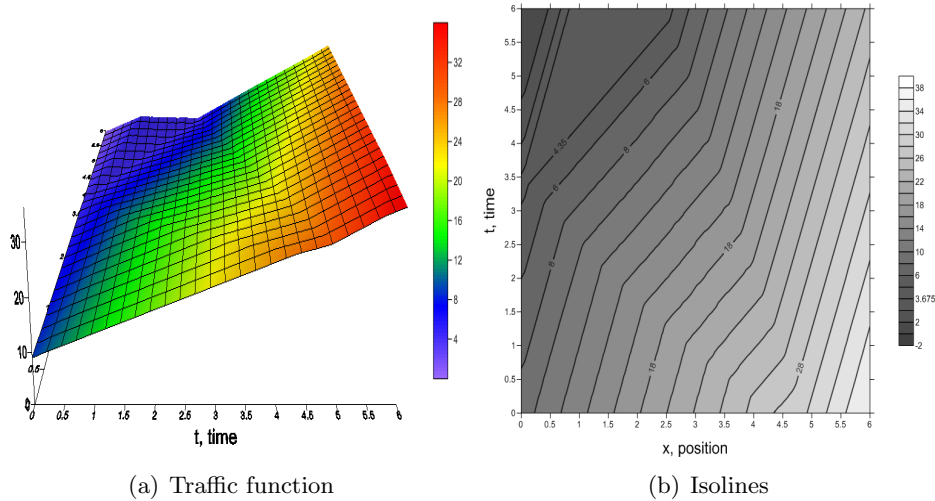


Figure 5: Solution of the Moskowitz problem with triangular fundamental diagram

Assume that the free-flow speed is a parameter that can vary in the range  $\nu \in [\nu_{min}, \nu_{max}] = [1.5, 3.0]$ . Consider a model where the variable speed limitations are applied locally in space and time. The fundamental diagram is then for  $\nu \in [\nu_{min}, \nu_{max}]$

$$h_1(t, x, \nu, p) = \begin{cases} h(\nu, \omega, p) & \text{if } (t, x) \in [0, 4.5] \times [0, 4] \\ h(\nu_{max}, \omega, p), & \text{otherwise} \end{cases}$$

where  $h$  is the triangular function defined by ( 4.20). The figure 6 illustrates the dependence of the fundamental diagram on the free-flow speed parameter.

The corresponding problem is now

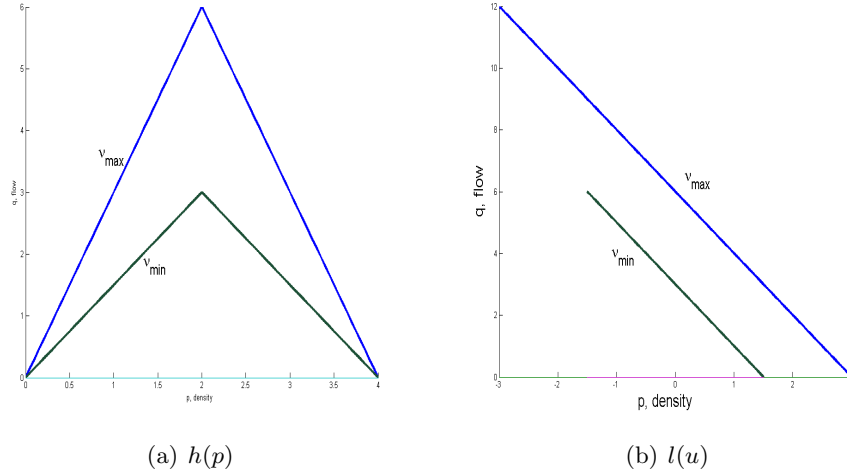


Figure 6: Triangular fundamental diagram with different free-flow speed values

$$\begin{cases} (i) & \mathbf{h}_1 \left( t, x, \nu, -\frac{\partial V(t, x, \nu)}{\partial x} \right) = \frac{\partial V(t, x, \nu)}{\partial t}, \quad (t, x) \in ]0, 6]^2, \quad \nu \in [\nu_{min}, \nu_{max}] \\ (ii) & V(t, x, \nu) \leq \mathbf{c}(t, x), \quad (t, x) \in [0, 6]^2, \quad \nu \in [\nu_{min}, \nu_{max}] \end{cases} \quad (4.34)$$

with the same target function  $c(t, x)$ . The figure 7 shows an example of the traffic function when the speed limit is fixed to  $\nu = 1.6$ .

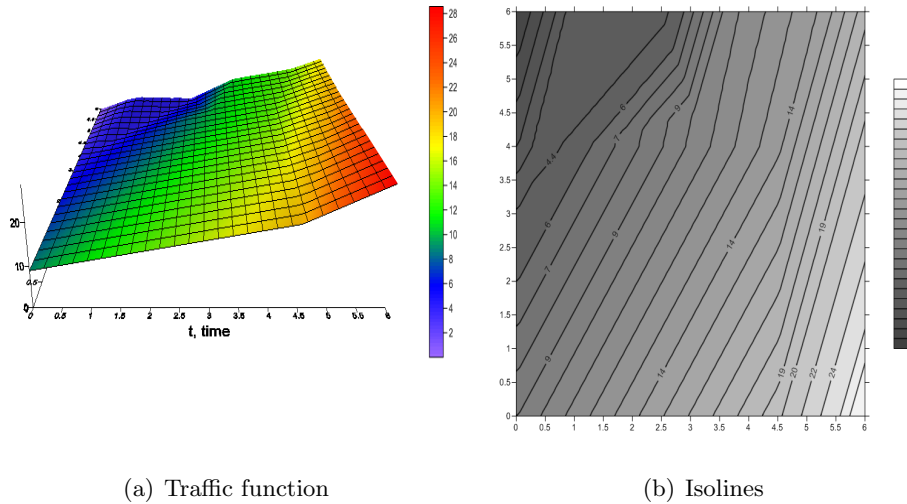


Figure 7: The traffic function with the free-flow speed locally limited to  $\nu = 1.6$

The comparison of iso-lines (see figure 8) of the traffic function show clearly the homogenization effect of the speed limit reduction. One can remark even that the travel times are reduced

for the congestion zone in the case of the smaller speed limit.

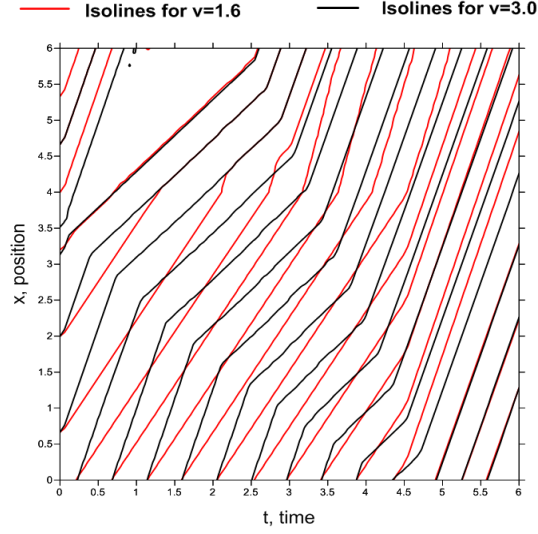


Figure 8: Triangular diagram: comparison of the isolines for two different values of the free-flow speed

#### 4.2.2 A local capacity reduction impact with variable speed limits

Consider a road section  $[0, 6]$  with a constant initial concentration  $C_0 = 1.5$ . Assume that an accident causes a local reduction of the capacity of the road on the interval  $[2.5, 3.5]$ : only one on the two lanes is free. Then the maximum capacity on this interval is  $0.5\omega = 2.0$ . Consider the Greenshields fundamental diagram (4.23) for this example. The fundamental diagram depends from the position  $x$  and we define the function

$$h_2(x, p) = \begin{cases} h(\nu, 0.5\omega, p) & \text{if } x \in [2.5, 3.5] \\ h(\nu, \omega, p), & \text{otherwise} \end{cases} \quad (4.35)$$

where  $h$  is the Greenshields function defined in (4.23).

Any information is available about the boundary condition. Then we will consider here a Cauchy problem:

$$\begin{cases} (i) & \mathbf{h}_2 \left( x, -\frac{\partial V(t, x)}{\partial x} \right) = \frac{\partial V(t, x)}{\partial t}, \quad (t, x) \in ]0, 6[^2 \\ (ii) & V(t, x) \leq \mathbf{c}(t, x), \quad (t, x) \in [0, 6]^2 \end{cases}$$

with the following target function  $c$ :

$$c(t, x) = c_0(t, x) \quad (4.36)$$

where the function  $c_0(t, x)$  corresponds to the initial condition

$$c_0(t, x) = \begin{cases} C_0(6.0 - x), & \text{if } t == 0 \\ +\infty, & \text{otherwise} \end{cases} \quad (4.37)$$

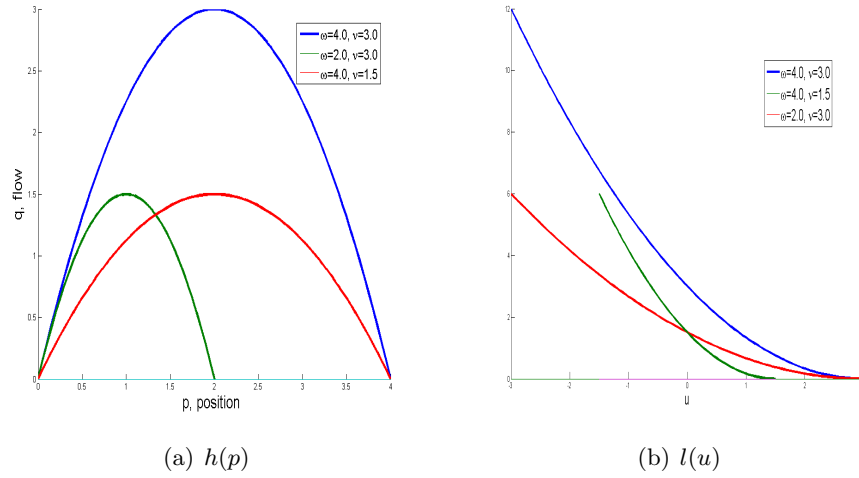


Figure 9: Greenshields fundamental diagram with different free-flow speed and maximal capacity values

The figure 10 shows, at the left, the traffic function computed by the viability algorithm and at the right the isolines ( that one can consider as a trajectories).

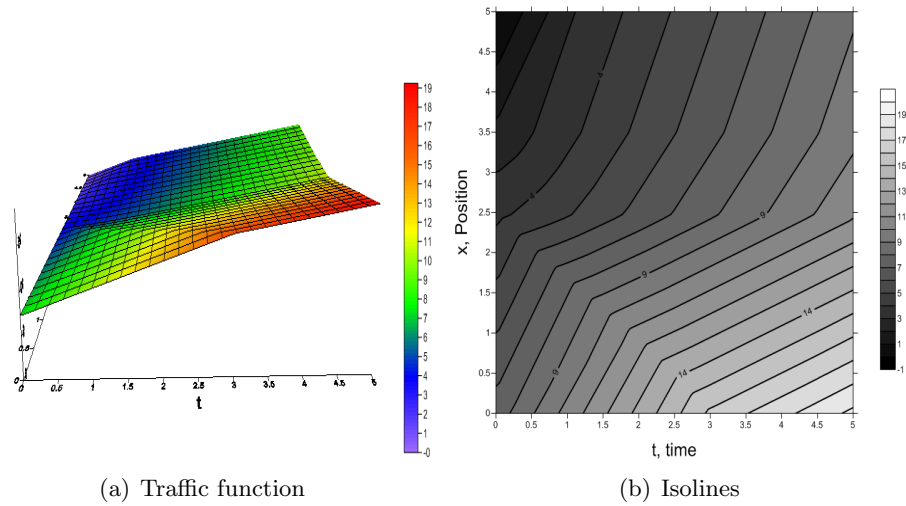


Figure 10: Solution of the Moskowitz problem

Assume that the free-flow speed is a parameter that can vary in the range  $\nu \in [\nu_{min}, \nu_{max}] = [1.5, 3.0]$ . Consider a model where the variable speed limitations are applied locally in space to limit the propagation of the bottleneck caused by the accident. The fundamental diagram is

then for  $v \in [\nu_{min}, \nu_{max}]$

$$h_3(x, v, p) = \begin{cases} h(\nu_{max}, 0.5\omega, p) & \text{if } x \in [2.5, 3.5] \\ h(v, \omega, p) & \text{if } x \in [0, 2.5[ \\ h(\nu_{max}, \omega, p), & \text{otherwise} \end{cases}$$

where  $h$  is the Greenshields function defined by ( 4.23). The figure 9 illustrates the dependence of the fundamental diagram on the free-flow speed parameter.

The corresponding problem is now

$$\begin{cases} (i) & \mathbf{h}_3 \left( x, \nu, -\frac{\partial V(t, x, \nu)}{\partial x} \right) = \frac{\partial V(t, x, \nu)}{\partial t}, \quad (t, x) \in ]0, 6]^2, \quad \nu \in [\nu_{min}, \nu_{max}] \\ (ii) & V(t, x, \nu) \leq \mathbf{c}(t, x), \quad (t, x) \in [0, 6]^2, \quad \nu \in [\nu_{min}, \nu_{max}] \end{cases} \quad (4.38)$$

with the same target function  $c(t, x)$ . The figure 11 shows an example of the traffic function when the speed limit is fixed to  $\nu = 1.6$ .

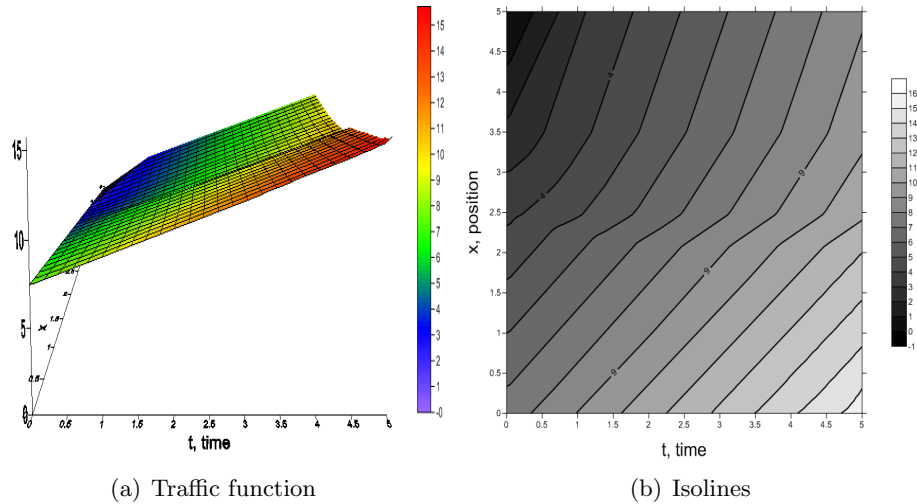


Figure 11: The traffic function with the free-flow speed locally limits to  $\nu = 1.6$

The comparison of iso-lines (see figure 12) of the traffic function show clearly the homogenization effect of the speed limit reduction. One can remark even that the travel times are reduced for the congestion zone in the case of the smaller speed limit.

#### 4.2.3 Locally congested initial traffic conditions

Consider a road section  $[0, 6]$  and assume that the initial concentration is a piecewise constant with a congested interval  $[3.0, 5.0]$  on which the concentration is  $C_1 = 3.0$ . Assume that otherwise on the road the initial concentration is  $C_0 = 0.9$ . Consider the Edie's fundamental diagram ( 4.26) for this example.

Any information is available about the boundary condition. Then we will consider here the Moskowitz problem ( 2.5): with the following target function  $c$ :

$$c(t, x) = c_0(t, x) \quad (4.39)$$

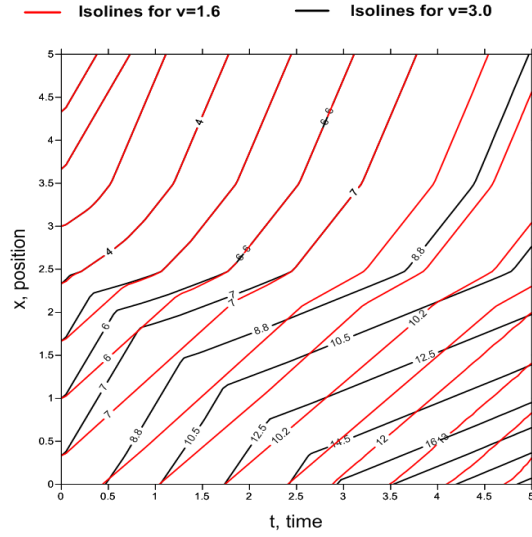


Figure 12: Greenshields diagram: comparison of the isolines for two different values of the free-flow speed

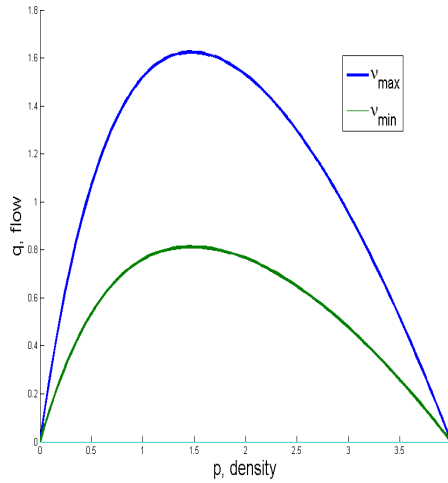


Figure 13: Edie's fundamental diagram with different free-flow speed and maximal capacity values

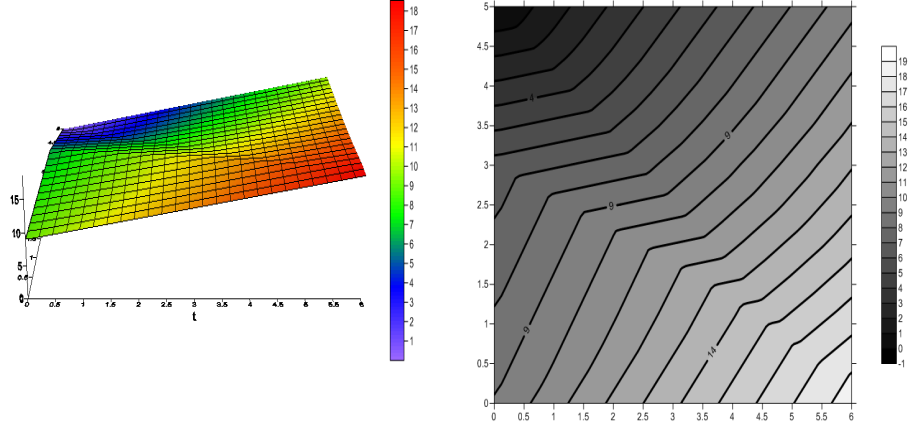
where the function  $c_0(t, x)$  corresponds to the initial condition

$$c_0(t, x) = \begin{cases} \gamma_0(x), & \text{if } t = 0 \\ +\infty, & \text{otherwise} \end{cases} \quad (4.40)$$

with

$$\gamma_0(x) = \begin{cases} 12.3 - 0.9x, & \text{if } x \in [0, 3[ \\ 3.2 * (6 - x), & \text{if } x \in [3, 5[ \\ 3.2 - 0.9(x - 5.0), & \text{if } x \in [5, 6] + \infty, \text{ otherwise} \end{cases}$$

The figure 14 shows, at the left, the traffic function computed by the viability algorithm and at the right the isolines ( that one can consider as a trajectories).



(a) Traffic function

(b) Isolines

Figure 14: Solution of the Moskowitz problem

Assume that the free-flow speed is a parameter that can vary in the range  $\nu \in [\nu_{min}, \nu_{max}] = [1.5, 3.0]$ . Consider a model where the variable speed limitations are applied locally in space to limit the retro propagation of the initial congested zone. The fundamental diagram is then for  $\nu \in [\nu_{min}, \nu_{max}]$

$$h_4(x, \nu, p) = \begin{cases} h(\nu, \omega, p) & \text{if } x \in [0, 3.0[ \\ h(\nu_{max}, \omega, p), & \text{otherwise} \end{cases}$$

where  $h$  is the Edie's function defined by ( 4.26). The figure 13 illustrates the dependence of the fundamental diagram on the free-flow speed parameter.

The corresponding problem is now

$$\begin{cases} (i) & \mathbf{h}_4 \left( x, \nu, -\frac{\partial V(t, x, \nu)}{\partial x} \right) = \frac{\partial V(t, x, \nu)}{\partial t}, \quad (t, x) \in ]0, 6]^2, \quad \nu \in [\nu_{min}, \nu_{max}] \\ (ii) & V(t, x, \nu) \leq \mathbf{c}(t, x), \quad (t, x) \in [0, 6]^2, \quad \nu \in [\nu_{min}, \nu_{max}] \end{cases} \quad (4.41)$$

with the same target function  $c(t, x)$ . The figure 15 shows an example of the traffic function when the speed limit is fixed to  $\nu = 1.6$ .

The comparison of iso-lines (see figure 16) of the traffic function show clearly the homogenization effect of the speed limit reduction. One can remark even that the travel times are reduced for the congestion zone in the case of the smaller speed limit.

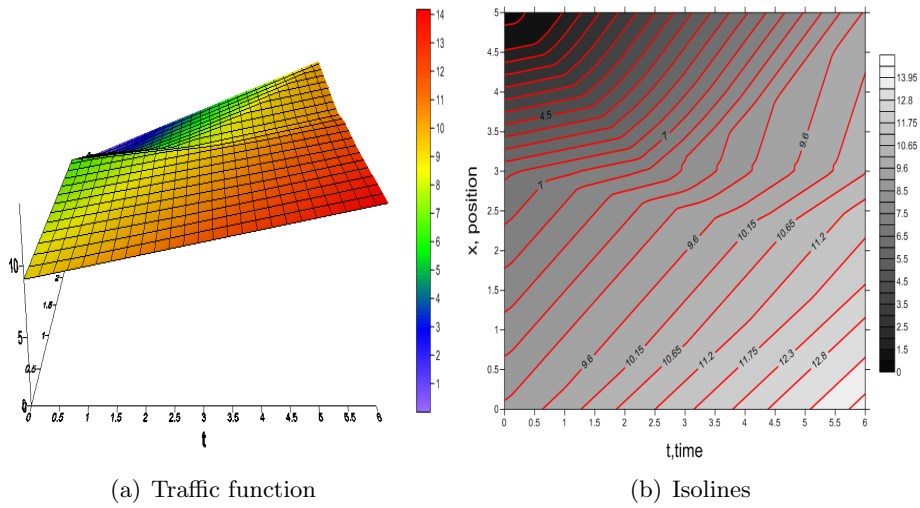


Figure 15: The traffic function with the free-flow speed locally limits to  $\nu = 1.6$

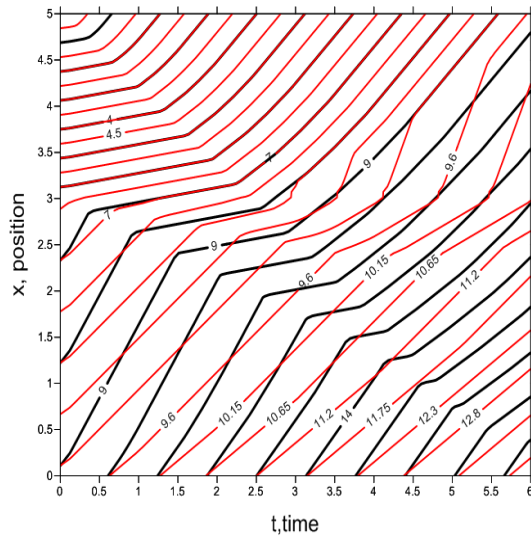


Figure 16: Edie's diagram: comparison of the isolines for two different values of the free-flow speed

## References

- [1] J.-P. Aubin. *Viability Theory*. Birkhäuser, Boston, 1991.
- [2] J.-P. Aubin, A. Bayen, and P. Saint-Pierre. *Viability Theory: New Directions*. Springer, 2011.
- [3] J.-P. Aubin and A. Cellina. *Differential inclusions*, volume 264 of *Comprehensive studies*

*in mathematics*. Springer, Berlin, Heidelberg, New York, Tokyo, 1984.

- [4] E. N. Barron and R. Jensen. Semicontinuous viscosity solutions for Hamilton-Jacobi equations with convex Hamiltonians. *Comm. Partial Differential Equations*, 15(12):1713–1742, 1990.
- [5] C. G. Claudel and A. M. Bayen. *Solutions to switched Hamilton-Jacobi equations and conservation laws using hybrid components*, volume 4981 of *Lecture Notes in Computer Science*, pages 105–115. Springer Verlag, Saint Louis, MO, 2008.
- [6] C. G. Claudel and A. M. Bayen. Convex formulations of data assimilation problems for a class of hamilton-jacobi equations. *SIAM Journal on Control and Optimization*, 2009.
- [7] C. G. Claudel and A. M. Bayen. Lax-hopf based incorporation of internal boundary conditions into hamilton-jacobi equation. part i: theory. *IEEE Transactions on Automatic Control*, 55(5):1142–1157, 2010.
- [8] C. G. Claudel and A. M. Bayen. Lax-hopf based incorporation of internal boundary conditions into hamilton-jacobi equation. part ii: Computational methods. *IEEE Transactions on Automatic Control*, 55(5):1158–1174, 2010.
- [9] C. Daganzo. A variational formulation of kinematic waves: basic theory and complex boundary conditions. *Transportation Research B*, 35B(2):187–196, 2005.
- [10] C. Daganzo. On the variational theory of traffic flow: well-posedness, duality and applications. *Networks and Heterogeneous Media*, 1:601–619, 2006.
- [11] L. C. Edie. Car following and steady state theory for non-congested traffic. *Operations Research*, 9:p66–76, 1961.
- [12] H. Frankowska. Lower semicontinuous solutions of Hamilton-Jacobi-Bellman equations. *SIAM J. Control Optim.*, 31(1):257–272, 1993.
- [13] H. Greeberg. An analysis of traffic flow. *perations Research*, 7(1):79–85, 1959.
- [14] B. D. Greenshields. A study of traffic capacity. *HRB Proc.*, 14:448–481, 1934.
- [15] A. M. Bayen J.-P. Aubin and P. Saint-Pierre. Dirichlet problems for some hamilton-jacobi equations with inequality constraints. *SIAM Journal on Control and Optimization*, 47(5):2348–2380, 2008.
- [16] M. J. Lighthill and G. B. Whitham. On kinematic waves: Ii. a theory of traffic flow on long crowded roads. *Proc. Royal Society*, 229(1178)(A):317–345, 1955.
- [17] G. Newell. Nonlinear effects in the dynamics of car following. *Operations Research*, 9, 1961.
- [18] P. I. Richards. Shock waves on the highway. *Operations Research*, 4:42–51, 1956.
- [19] R. T. Underwood. Speed, volume and density relationships, quality and theory of traffic flow. *Yale Bureau of Highway Traffic*, pages 141–88, 1961.